

Application of PAN/ α -Fe₂O₃-Bentonite as A Photocatalytic Membrane for The Photodegradation of Methylene Blue

Dina Wardani Sitompul, Tetty Kemala, Noviyan Darmawan

Department of Chemistry, Faculty of Mathematics and Natural Sciences, IPB University
Jl. Raya Dramaga Kampus IPB Dramaga Bogor, 16680, Indonesia

*Corresponding author: tettykemala@apps.ipb.ac.id

Received: October 2022; Revision: March 2023; Accepted: March 2023; Available online: May 2023

Abstract

The intricate molecular structure of the dyes in wastewater makes it difficult to biodegrade, which could harm the environment. Currently, semiconductor-based photocatalytic methods are being developed to remove dyes from water. In this study, the α -Fe₂O₃-bentonite photocatalyst was synthesized by mechanical milling and immobilized in polyacrylonitrile (PAN) membrane by phase inversion. Analysis of the composition and surface morphology of the synthesized samples was carried out by FTIR, XRD, and EDX. The performance of the photocatalytic membrane was studied by investigating the removal of methylene blue (MB). Photocatalytic membrane with 2% α -Fe₂O₃-bentonite had the best performance in removing MB (10 ppm) that reached 99.84% at pH 11.5 with an irradiation time of 300 minutes under direct sunlight. The reuse cycle of the photocatalytic membrane was also carried out and the results showed that there is no significant change in the photodegradation efficiency after 5 cycles. Photocatalyst immobilization on PAN membranes is proven to overcome the post-recovery problem of photocatalysts and making easier to reuse. The photocatalyst membrane synthesized in this study can be used as an alternative for removing dyes from water.

Keywords: α -Fe₂O₃; bentonite; photocatalyst membrane; methylene blue

DOI: 10.15408/jkv.v9i1.28635

1. INTRODUCTION

One of the substances that significantly contribute to the contamination of the aquatic environment is the presence of synthetic dyes in industrial effluent. Synthetic dyes are a class of dispersed chemical compounds that are challenging for nature to break down. They pose risks to both human health and the environment (Lellis et al., 2019). The aesthetic value of water bodies is significantly diminished by dye pollution, which also increases the need for biochemical and chemical oxygen, hinders photosynthesis, prevents plant growth, enters the food chain, results in recalcification and bioaccumulation, and make water more toxic, mutagenic, and carcinogenic (Al-Tohamy et al., 2022).

Effective and environmentally friendly dye waste treatment techniques are continuously being developed due to their negative impacts on the environment, human

health, and natural water resources. Numerous studies have been conducted on the technology for treating wastewater that contains dyes using physical methods (adsorption), chemical methods (photo-Fenton), and biological methods (anaerobic, aerobic) (Periyasamy et al., 2018). However, these techniques have certain downsides, including the creation of hazardous byproducts, the formation of sludge, the need for high temperatures, and their restricted use for chemical oxygen demand (COD) and biological oxygen demand (BOD) (Al-Tohamy et al., 2022).

In recent years, photocatalysis based on semiconductor materials is considered a promising alternative technology for the treatment of industrial wastewater containing dyes because it is low cost, environmentally friendly, does not produce harmful secondary products, is sustainable and energy efficient (Chiu et al., 2019). Metal oxides such as TiO₂

and ZnO are the most explored semiconductor materials in photocatalyst applications for environmental remediation. However, these materials have drawbacks such a large band gap energy and poor light absorption, thus their activity is restricted to sunlight's UV radiation (Nemiwal et al., 2021).

The hematite (α -Fe₂O₃) semiconductor has advantages over TiO₂, ZnO, and other materials in the utilization of solar energy for photocatalytic applications because it has a lower band gap of approx 2.0-2.2 eV. Additionally, α -Fe₂O₃ is abundantly available, non-toxic, and recyclable, making it a potential substance for use as a photocatalyst (Hitam and Jalil 2020). Nonetheless, α -Fe₂O₃ requires modification with other materials in order to enhance performance due to its high rate of electron-hole recombination. Modification of α -Fe₂O₃ with bentonite has been reported by Suprihatin et al. (2019) can increase the surface area, active site, and suppress the rate of charge recombination so as to improve the photocatalytic performance of α -Fe₂O₃.

Bentonite is a natural clay type material consisting of two silica tetrahedral sheets and one central alumina octahedral sheet. The application of bentonite as adsorbents and composite supports is quite common due to its large surface area, mechanical properties, high thermal stability, and widespread availability in nature (Bananezhad et al., 2019). The α -Fe₂O₃-bentonite nanocomposite has been reported as an effective photocatalyst in removing indigo carmine (Bananezhad et al., 2019), remazol brilliant blue (Riskiani et al., 2018; Suprihatin et al., 2019). Though remarkably effective, utilizing photocatalyst in suspension to treat wastewater has a drawback, specifically the requirement for post-recovery following the photocatalysis process. The necessity to separate the photocatalyst from the suspension increases operational costs and decreases processing efficiency. Immobilizing photocatalysts on supports or thin films is a viable approach to solving this issue. Additionally, by loading the photocatalyst on or at the membrane surface, photocatalyst regeneration would be easily implemented (Nasrollahi et al., 2021).

The challenge of photocatalyst recovery after being utilized in photocatalytic processes has already been addressed by modified photocatalysts into membrane (Mpelane et al., 2020). In this study, the mechanical milling

approach was used in a planetary ball mill to quickly and economically synthesize α -Fe₂O₃-bentonite nanocomposite photocatalyst. The produced α -Fe₂O₃-bentonite particles were immobilized on polyacrylonitrile (PAN) membrane to facilitate easier reuse of the photocatalyst by phase inversion technique. PAN is a versatile polymer exhibiting high chemical, mechanical, and thermal membrane-forming properties as well as solvent resistance that has been extensively used as membrane material for water treatment (Karimnezhad et al., 2019). The photocatalytic activity of the newly developed photocatalyst membrane evaluated through the degradation of the methylene blue (MB). According to the literature, membrane photocatalyst PAN α -Fe₂O₃-bentonite has never been produced. Modification of photocatalysts into membranes is expected to overcome post-photocatalyst problems so as to increase the effectiveness and efficiency of α -Fe₂O₃-bentonite photocatalyst to degrade textile dyes.

2. MATERIALS AND METHODS

Materials and Tools

The following chemicals and materials were utilized in this study: ferrous sulphate salt (Fe₂SO₄·7H₂O) (Pudak Scientific), hydrochloric acid (37%, Merck), sodium hydroxida (Merck), ammonia solution (25%, Merck), dimethyl sulfoxide (DMSO) (Merck), ethanol (99.9%, Merck), polyacrylonitrile (PAN) (Mw 150,000, Future Chemical, China), commercial bentonite clay (Pudak Scientific), methylene blue (Merck), and distilled water.

To measure the concentration of methylene blue, a Shimadzu UV mini-1240 UV-Vis spectrophotometer was used. Fourier Transform Infrared Spectroscopy (Spectrum One spectrometer, PerkinElmer), X-Ray Diffraction (D2 Phaser, Bruker) and Energy Dispersive X-Ray (Phenom ProX) were utilized for characterization of synthesis result.

Synthesis of α -Fe₂O₃ Nanoparticles

Nanoparticles α -Fe₂O₃ was synthesized by dissolving 5 g ferrous sulfate (Fe₂SO₄·7H₂O) in 100 mL distilled water. After 30 minutes of stirring at 60 °C, 50 mL of ammonia solution (pH≈11) was added to the mixture in order to precipitate the nanoparticles. The product was filtered, rinsed with ethanol and distilled water, then dried. The final product was a brick red

powder which was calcined at 600 °C for 3 hours (Sharma et al., 2021).

Synthesis of Nanobentonite

A total of 5 g of bentonite powder was added in 100 mL distilled water followed by the addition of 50 mL HCl (pH \approx 4) to form a suspension. After being continually stirred and heated for 2 hours at 65 °C, the suspension was filtered. The product was dried and then calcined at 400 °C for 3 hours to obtain a white bentonite nanoparticle powder (Sharma et al., 2021).

Synthesis of α -Fe₂O₃-Bentonite Nanocomposite

The synthesized nanoparticles of α -Fe₂O₃ and bentonite were mixed with a weight ratio of 4:1, then ground using a planetary ball mill for 2 hours at a speed of 350 rpm (the ratio of the ball to the sample is 7:1) (Lubis et al., 2019).

Immobilization of α -Fe₂O₃-Bentonite Nanocomposite on PAN

The α -Fe₂O₃-bentonite nanocomposite with different concentrations were immobilized on polyacrylonitrile membranes to determine the optimal photocatalyst mass. A total of 1.5 g of PAN was dissolved in 7 mL of DMSO while stirring. Different concentrations of the photocatalyst Fe₂O₃-bentonite (0%, 1%, 1.5%, and 2%) were added to a different beaker containing dissolved PAN, and then homogenized by stirring and sonication. Afterwards, the polymer solution was spread to cylindrical glass plates with a 7 cm diameter and aged in the open air for 10 minutes. The glass plates were soaked in a coagulation bath with a water to ethanol ratio of 5:1. In preparation for additional testing, the produced photocatalytic PAN membranes were rinsed and kept in deionized water (Mpelane et al., 2020).

Characterization

The functional groups on the prepared nanocomposite and the photocatalytic membranes were identified using a Perkin Elmer Fourier transform infrared (FTIR) spectrometer (Spectrum One). The range of FTIR spectra were obtained in 4000–400 cm⁻¹. The D2 Phaser X-ray Diffraction (XRD) instrument (Bruker) was used to probe the crystallinity of the fabricated photocatalysts. Energy Dispersive X-Ray (Phenom ProX) was

utilized for elemental composition analysis of synthesized products.

Evaluation of Photocatalytic Efficiency of PAN/ α -Fe₂O₃-Bentonite Membrane

The photocatalytic activity of the prepared PAN/ α -Fe₂O₃-bentonite membrane was evaluated in MB dye degradation. The effect of photocatalyst loading on MB degradation was evaluated by varying the mass of α -Fe₂O₃-bentonite nanocomposite immobilized on the PAN membrane. Membranes with 0%, 1%, 1.5%, and 2% of α -Fe₂O₃-bentonite were prepared by adding the photocatalyst with 1.5 g of PAN membrane. Furthermore, a reactor with PAN/Fe₂O₃-bentonite membrane filled with 100 mL of MB solution at a concentration of 10 ppm. At intervals of 50 minutes, aliquots from each reactor were collected to measure the concentration change using UV-Vis spectroscopy during 300 minutes of UV radiation (Mpelane et al., 2020). The percent degradation (%D) equation is then applied to calculate the concentration value.

The effect of pollutant concentration was carried out by varying the initial concentration (10, 20 and 30 ppm) of MB. Effect of pH on MB photodegradation rate evaluated by varying the pH of the solution under acidic, neutral and basic conditions. The pH levels were adjusted using sodium hydroxide and hydrochloric acid to 3.5, 7, and 11.5 respectively. The effect of light sources on the photodegradation rate of MB was also evaluated by conducting experiments on different radiation sources using UV lamp and sunlight. All UV light studies were conducted using a UV lamp within a radiation box. The lamp is placed at a distance of 15 cm above the reactor. To ensure the repeatability of the membrane, each experiment was conducted in 5 times.

3. RESULTS AND DISCUSSION

Fourier Transform Infrared Spectroscopy (FTIR) Spectrum

Figure 1 shows the FTIR spectra of (a) bentonite, (b) α -Fe₂O₃, (c) nanocomposite α -Fe₂O₃-bentonite, (d) PAN, and (e) PAN/ α -Fe₂O₃-bentonite respectively. In the bentonite spectra (**Figure 1a**), the extended absorption band at 3487 cm⁻¹ represents the stretching band for O-H and H₂O molecular hydrogen bonds. The H-O-H absorption band is detected as a weak peak at 1639 cm⁻¹ while Si-

O-Si absorption band is represented by the broad peak in 1092 cm^{-1} . Stretching of the Si-O quartz and silica lead to the modest peak that appeared at 795 cm^{-1} (Bananezhad et al., 2019). The strain vibration of the Fe-O is characterized by strong peaks in the $\alpha\text{-Fe}_2\text{O}_3$ spectra (Figure 1b) at 549 and 481 cm^{-1} (Fouad et al., 2019). The spectra of $\alpha\text{-Fe}_2\text{O}_3$ -bentonite (Figure 1c) at 1088 cm^{-1} and 794 cm^{-1} exhibit an absorption band of Si-O-Si groups and Si-O stretching originating from bentonite.

The FTIR spectra of PAN (Figure 1d) and PAN/ $\alpha\text{-Fe}_2\text{O}_3$ -bentonite membranes (Figure 1e) revealed peaks at 1459 cm^{-1} and 2932 cm^{-1} , which corresponded to the bending vibrations and stretching of the C-H bond of the

methyl group in PAN, respectively. The peak at 2241 cm^{-1} is responsible for strain vibration of the $\text{C}\equiv\text{N}$ group. The C-H group on the type III carbon chain provides the buckling vibration at 1369 cm^{-1} . The C=C bond strain of the vinyl acetate group is related to the peak at 1625 cm^{-1} . The strain vibration of C=O from the carbonyl group appears at 1735 cm^{-1} (Karimnezhad et al., 2019). The characteristic peak in the PAN/ $\alpha\text{-Fe}_2\text{O}_3$ -bentonite spectrum appears at 537 cm^{-1} which is the Fe-O group strain of the nanocomposite. The appearance of all peaks at certain wavenumber indicates the presence of functional groups that are expected in each synthesized sample.

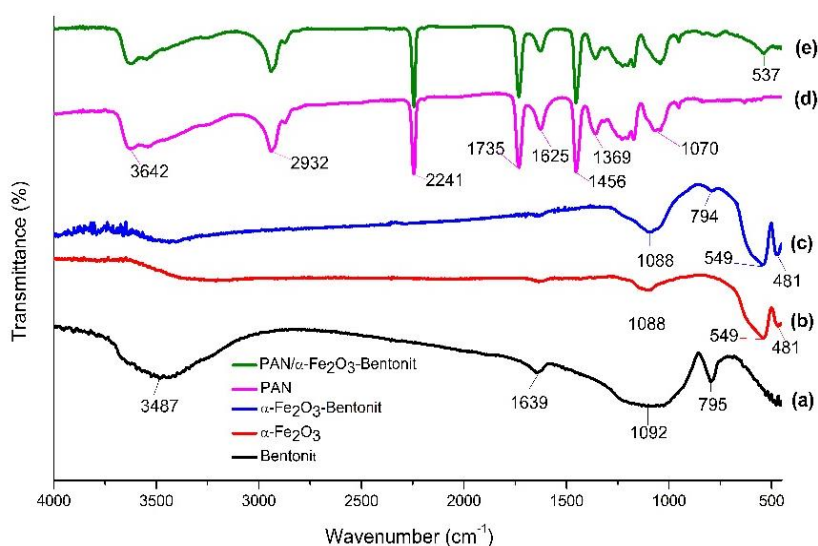


Figure 1. FTIR spectra of (a) bentonite, (b) $\alpha\text{-Fe}_2\text{O}_3$, (c) $\alpha\text{-Fe}_2\text{O}_3$ -bentonite, (d) PAN, (e) PAN/ $\alpha\text{-Fe}_2\text{O}_3$ -bentonite

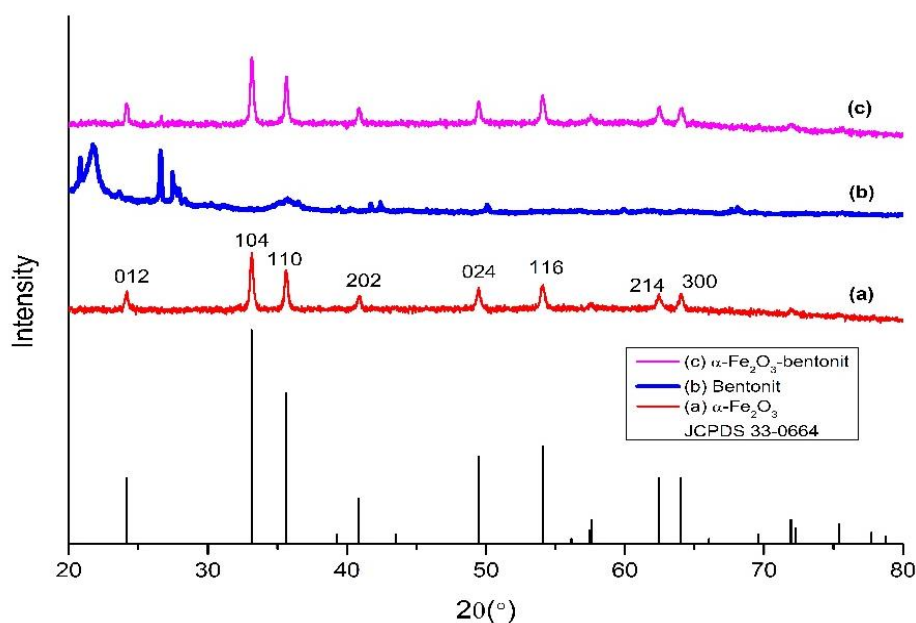


Figure 2. XRD pattern of (a) $\alpha\text{-Fe}_2\text{O}_3$, (b) bentonite and (c) $\alpha\text{-Fe}_2\text{O}_3$ -bentonite

X-Ray Diffraction (XRD) Spectrum

Figure 2 shows the X-ray diffraction pattern of (a) α -Fe₂O₃, (b) bentonite and (c) α -Fe₂O₃-bentonite nanocomposite. XRD pattern for α -Fe₂O₃ (**Figure 2a**) obtained 2 θ peaks at: 24.16°, 33.21°, 35.67°, 40.91°, 49.47°, 54.09°, 62.43°, and 64.03° correspond to crystal peaks 012, 104, 110, 202, 024, 116, 214, and 300. According to JCPDS No. 33-0664, the acquired XRD pattern corresponds with typical α -Fe₂O₃. The XRD pattern of bentonite (**Figure 2b**) reveals that reflections related to quartz (SiO₂) emerge at 2 θ =20.82°, 24.62° and 40.42° (JCPDS no. 96-900-5022). The diffraction pattern of the α -Fe₂O₃-bentonite nanocomposite (**Figure 2c**) shows the existence of α -Fe₂O₃ peaks that are identical with JCPDS No. 33-0664 as well as the appearance of SiO₂ peaks from the bentonite albeit at a lower intensity. Each of the synthetic materials exhibited characteristic peaks that corresponded to those reported in the literature (Lubis et al., 2019; Suprihatin et al., 2019). The average crystal size of α -Fe₂O₃, bentonite and α -Fe₂O₃-bentonite nanocomposite was calculated using the Debye Scherer formula. The average crystal size for α -Fe₂O₃, bentonite, and α -Fe₂O₃-bentonite nanocomposites were 47.09, 46.88 and 49.39 nm respectively. The result of the crystal size computation demonstrated that each

of the materials produced for this study featured in nanoscale.

Analysis Result of Energy Dispersion X-Ray Spectroscopic (EDX)

The analysis of the composition of the elements contained in the nanocomposite and the synthesized membrane are shown in **Figure 3**. The EDX spectrum of the α -Fe₂O₃-bentonite nanocomposite (**Figure 3a**) is consistent with the findings of the XRD study, which reveals that Fe and O are the constituent elements of α -Fe₂O₃, which has the highest proportion of atomic weight. The elements Si, C, Al and Mg are the constituent elements of bentonite which are found in low percentages. **Figure 3b** shows the EDX spectrum of the PAN/ α -Fe₂O₃-bentonite membrane. The most dominant elements contained in the membrane are C, N and O which are the main constituents of polyacrylonitrile. The presence of Fe, Si, Mg, and Al elements were also found in the membrane with a lower percentage. This supports the findings of the FTIR analysis of the photocatalyst membrane, which revealed the presence of the components of the nanocomposite. The elemental percentages which are represented in the synthetic nanocomposite and photocatalytic membrane are listed in **Table 1**.

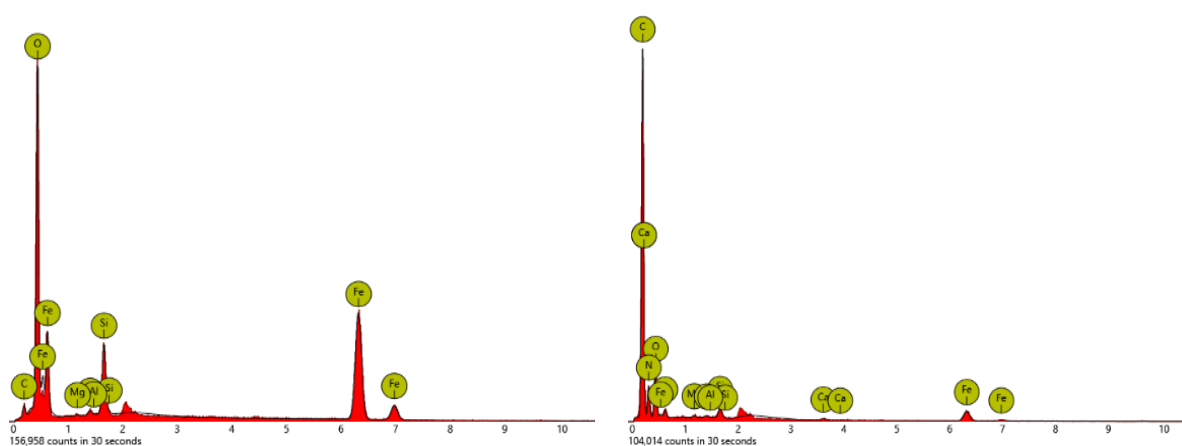


Figure 3. EDX Spectrum of (a) α -Fe₂O₃-bentonite and (b) PAN/ α -Fe₂O₃-bentonite

Table 1. Percentage of atomic weight of elements present in α -Fe₂O₃-bentonite and PAN/ α -Fe₂O₃-bentonite

Element (% Atom)	Fe	O	Si	C	N	Mg	Al
α -Fe ₂ O ₃ -bentonite	31.39	54.33	5.94	7.71	-	0.15	0.49
PAN / α -Fe ₂ O ₃ -bentonite	1.32	15.56	0.26	57.18	25.51	0.07	0.05

The Photocatalytic Activity of PAN/ α -Fe₂O₃-Bentonite Membrane

The photocatalytic activity of the synthesized PAN/ α -Fe₂O₃-bentonite membrane was evaluated in the degradation of MB dye. To determine the optimum operating conditions for the PAN/ α -Fe₂O₃-bentonite membrane, parameters such photocatalyst dosage on the membrane, pH, initial dye concentration, and radiation source were evaluated. The effect of photocatalyst loading on MB degradation of various parameters is shown in **Figure 4**.

Figure 4a shows the effect of photocatalyst loading on MB degradation as evaluated by varying the concentration of α -Fe₂O₃-bentonite nanocomposite immobilized on the PAN membrane (0%, 1%, 1.5%, and 2%). In the experiment, a membrane without any photocatalyst was employed as a control. The results showed that the rate of photodegradation increased as the concentration of photocatalyst on the PAN membrane improved. The membrane with 2% α -Fe₂O₃-bentonite demonstrated the best photocatalytic activity in degrading MB (73.99%). In this study, the highest concentration of photocatalyst that could be immobilized without compromising membrane integrity was 2%.

The effect of the initial concentration on the rate of photodegradation was studied by varying the initial concentrations of 10, 20, and 30 ppm of MB. **Figure 4b** shows that as concentration increases, the percentage of photodegradation decreases. The highest

degradation percentage (73.99%) was achieved with MB dye at an initial concentration of 10 ppm. When the MB concentration was increased to 20 and 30 ppm, the photodegradation efficiency dropped dramatically to 36.78% and 34.97%, respectively. The decrease in photocatalytic activity can be attributed to the effect of reduced light penetration as dye concentration increases, resulting in a less number of photogenerated electrons and holes (Mpelane et al., 2020).

Figure 4c depicts the effect of pH on the rate of MB dye photodegradation using a 2% PAN/ α -Fe₂O₃-bentonite photocatalyst membrane with an initial dye concentration of 10 ppm. The results showed that the photocatalyst membrane PAN/ α -Fe₂O₃-bentonite worked more effectively at pH 11.5, with photodegradation efficiency reaching 86.30%, compared to pH 3.5, where photodegradation efficiency only reached 43.45%. This is due to the fact that the electrostatic interaction between the positively charged MB dye and the photocatalyst surface tends to be higher in an alkaline environment since the photocatalyst membrane's surface has a tendency to be negatively charged (Sharma et al., 2021). On the other hand, in an acidic environment, the hematite-based photocatalyst's surface will become positively charged (FeOH⁺). This leads to protons competing with cationic dyes for the available adsorption sites, which reduces adsorption. This condition reduced the rate of photodegradation of MB (Sharma et al., 2021).

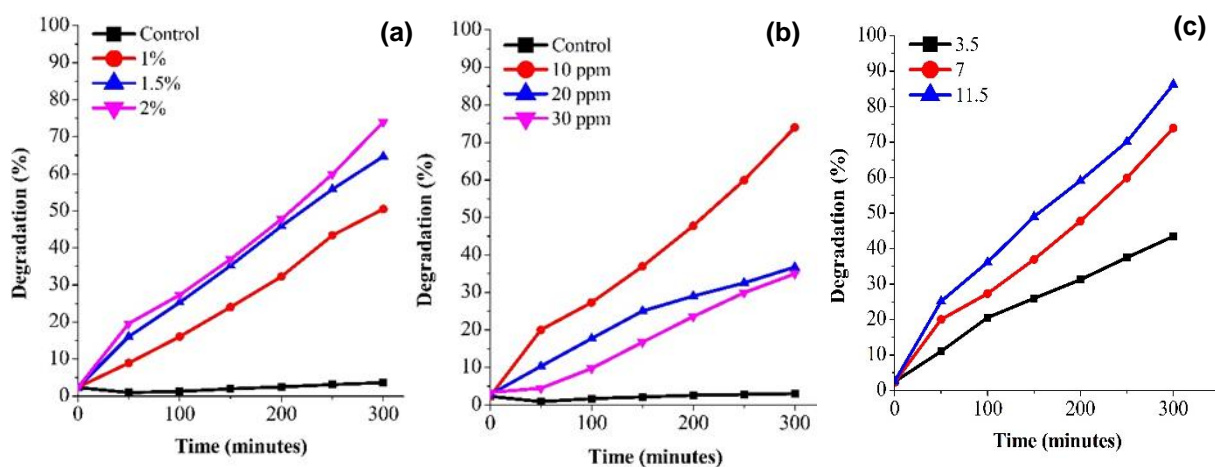


Figure 4. Plot of MB dye degradation (%) to study the effect of photocatalyst load (a) initial concentration of MB (b), and pH (c) using UV radiation

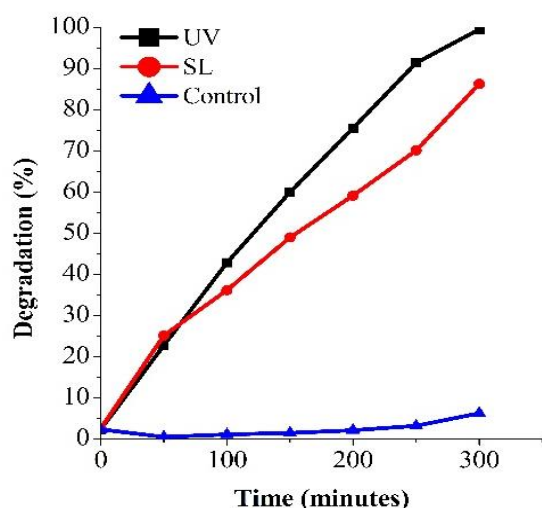


Figure 5. Effect of light source on MB

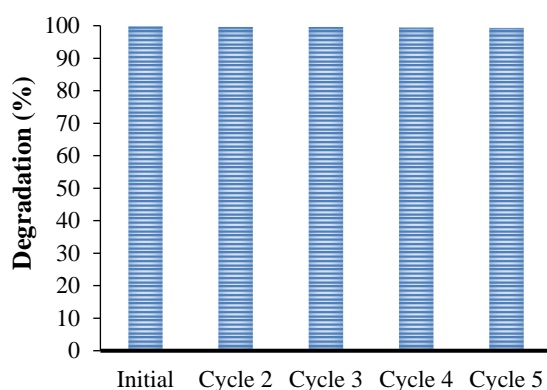


Figure 6. Reusability cycles in the MB photodegradation using 2% PAN/ α -Fe₂O₃-bentonite

Figure 5 shows the influence of a light source on MB dye degradation using 2% PAN/ α -Fe₂O₃-bentonite membrane. The experiment was conducted with sunlight and UV light under optimal conditions (10 ppm MB, pH 11.5). The photodegradation efficiency obtained by irradiating sunlight and UV light were 99.84% and 86.30%, respectively. These findings show that the 2% PAN/ α -Fe₂O₃-bentonite membrane works better under the sun rather than under UV light. Sunlight has a wider range of light than UV rays, which only cover 5% of the sun's spectrum. This enables the α -Fe₂O₃-modified bentonite to have photocatalytic activity in visible light, which offers a broader spectrum coverage. The PAN/ α -Fe₂O₃-bentonite photocatalyst synthesized in this study proved to be effective in removing MB in water. Further investigation into the reuse of photocatalyst membranes was carried out. The results obtained are shown in **Figure 6**. After five cycles of membrane reuse,

there was no significant change in photocatalyst performance. This proves that the PAN/ α -Fe₂O₃-bentonite photocatalyst membrane is effective in removing dyes from water contaminated with textile dyes.

4. CONCLUSION

The α -Fe₂O₃-bentonite nanocomposite has been successfully synthesized and immobilized on a polyacrylonitrile membrane. The synthesized PAN/ α -Fe₂O₃-bentonite membrane photocatalyst performed effectively, with a photodegradation efficiency of 99.84%, in the degradation of MB dye. This study determined that the optimum load of α -Fe₂O₃-bentonite photocatalyst that can be charged on the PAN membrane is 2%. The optimum performance of the photocatalytic membrane PAN/ α -Fe₂O₃-bentonite occurs in alkaline solution with an initial concentration of MB 10 ppm under the sunlight irradiation. Immobilization of α -Fe₂O₃-bentonite nanocomposite into the membrane can overcome the problem of photocatalyst post-recovery, allowing them to be reused more easily. The results of five cycles of membrane reuse proved that the synthesized photocatalytic membrane could be reused without significantly reducing photocatalyst performance.

REFERENCES

- Al-Tohamy, R., Ali, S. S., Li, F., Okasha, K. M., Mahmoud, Y. A. G., Elsamahy, T., Jiao, H., Fu, Y., Sun, J. (2022). A critical review on the treatment of dye-containing wastewater: ecotoxicological and health concerns of textile dyes and possible remediation approaches for environmental safety. *Ecotoxicology and Environmental Safety* 231:113160. doi: 10.1016/j.ecoenv.2021.113160.
- Bananezhad, B., Islami, M. R., Ghonchepour, E., Mostafavi, H., Tikdari, A. M., Rafiei, H. R. (2019). Bentonite clay as an efficient substrate for the synthesis of the super stable and recoverable magnetic nanocomposite of palladium (Fe₃O₄/Bentonite-Pd). *Polyhedron* 162:192–200. doi: 10.1016/j.poly.2019.01.054.
- Chiu, Y. H., Chang, T. F. M., Chen, C. Y., Sone, M., Hsu, Y. J. (2019). Mechanistic insights into photodegradation of organic dyes using

- heterostructure photocatalysts. *Catalysts* 9(5). doi: 10.3390/catal9050430.
- Fouad, D. E., Zhang, C., El-Didamony, H., Yingnan, L., Mekuria, T. D., Shah, A. H. (2019). Improved size, morphology and crystallinity of hematite ($\alpha\text{-Fe}_2\text{O}_3$) nanoparticles synthesized via the precipitation route using ferric sulfate precursor. *Results in Physics* 12(November 2018):1253–61. doi: 10.1016/j.rinp.2019.01.005.
- Hitam, C. N. C., Jalil, A. A. (2020). A review on exploration of Fe_2O_3 photocatalyst towards degradation of dyes and organic contaminants. *Journal of Environmental Management* 258(October 2019):110050. doi: 10.1016/j.jenvman.2019.110050.
- Karimnezhad, H., Navarchian, A. H., Gheinani, T. T., Zinadini, S. (2019). Incorporation of iron oxyhydroxide nanoparticles in polyacrylonitrile nanofiltration membrane for improving water permeability and antifouling property. *Reactive and Functional Polymers* 135(December 2018):77–93. doi: 10.1016/j.reactfunctpolym.2018.12.016.
- Lellis, B., Fávaro-Polonio, C. Z., Pamphile, J. A., Polonio, J. C. (2019). Effects of textile dyes on health and the environment and bioremediation potential of living organisms. *Biotechnology Research and Innovation* 3(2):275–90. doi: 10.1016/j.biori.2019.09.001.
- Lubis, S., Sheilatina, Sitompul, D. W. (2019). Photocatalytic degradation of indigo carmine dye using $\alpha\text{-Fe}_2\text{O}_3$ /bentonite nanocomposite prepared by mechanochemical synthesis. *IOP Conference Series: Materials Science and Engineering* 509(1). doi: 10.1088/1757-899X/509/1/012142.
- Mpelane, A., Katwire, D. M., Mungondori, H. H., Nyamukamba, P., Taziwa, R. T. (2020). Application of novel C-TiO₂-CFA/PAN photocatalytic membranes in the removal of textile dyes in wastewater. *Catalysts* 10(8):1–17. doi: 10.3390/catal10080909.
- Nasrollahi, N., Ghalamchi, L., Vatanpour, V., Khataee, A. (2021). Photocatalytic-membrane technology: a critical review for membrane fouling mitigation.” *Journal of Industrial and Engineering Chemistry* 93:101–16.
- Nemiwal, M., Zhang, T. C., Kumar, D. (2021). Recent progress in G-C₃N₄, TiO₂ and ZnO based photocatalysts for dye degradation: strategies to improve photocatalytic activity. *Science of the Total Environment* 767:144896. doi: 10.1016/j.scitotenv.2020.144896.
- Periyasamy, A. P., Ramamoorthy, S. K., Rwawiire, S., Zhao, Y. (2018). Sustainable Wastewater Treatment Methods for Textile Industry. Pp. 21–87. Switzerland: Spring Nature.
- Riskiani, E., Suprihatin, I. E., Sibarani, J. (2018). Fotokatalis bentonit- Fe_2O_3 untuk degradasi zat warna remazol brilliant blue. *Cakra Kimia*, 7(1):46–54.
- Sharma, P., Yadav, V., Kumari, S., Ghosh, D., Rawat, P., Vij, A., Srivastava, C., Saini, S., Sharma, V., Hassan, M. I., Majumder, S. (2021). Deciphering the potent application of nanobentonite and $\alpha\text{-Fe}_2\text{O}_3$ /bentonite nanocomposite in dye removal: revisiting the insights of adsorption mechanism. *Applied Nanoscience* (0123456789). doi: 10.1007/s13204-021-01927-z.
- Suprihatin, I. E., Sibarani, J., Sulihingtyas, W. D., Ariati, K. (2019). Photodegradation of remazol brilliant blue using Fe_2O_3 intercalated bentonite. *Journal of Physics: Conference Series* 1341(3):6–11. doi: 10.1088/1742-6596/1341/3/032028.